Published in final edited form as:
Matrix Biol. 2012 March ; 31(2): 120–134. doi:10.1016/j.matbio.2011.12.002.

The γ3 Chain of Laminin is Widely But Differentially Expressed in Murine Basement Membranes: Expression and Functional Studies

Yong N. Li[1,#], **Stephanie Radner**[1], **Margaret M. French**[2], **Germán Pinzón-Duarte**[3], **Gerard H. Daly**[1], **Robert E. Burgeson**[2], **Manuel Koch**[2,4], and **William J. Brunken**[1,2,3,*]

[1]Sackler School for Biomedical Sciences, Tufts University School of Medicine, 136 Harrison Avenue, Boston, MA 02111

[2]Cutaneous Biology Research Center, Massachusetts General Hospital, Harvard Medical School, Charlestown, MA 02129

[3]SUNY Eye Institute and the Departments of Ophthalmology and Cell Biology, SUNY Downstate Medical Center, Brooklyn, NY 11203

[4]Institute for Oral and Musculoskeletal Biology, Center for Biochemistry and Center for Molecular Medicine Cologne, University of Cologne, Joseph-Stelzmann Street 52, 50931 Cologne, Germany

Abstract

Laminins are heterotrimeric extracellular glycoproteins found in, but not confined to, basement membranes (BMs). They are important components in formation of the molecular networks of BMs as well as in cell polarity, cell differentiation and tissue morphogenesis. Each laminin is composed by an α, a β and a γ chain. Previous studies have shown that the γ3 chain is partnered with either the β1 chain (in placenta) or β2 chain (in the CNS) (Libby et al., 2000). Several studies, including our own, suggested that the γ3 chain is expressed in both apical and basal compartments (Gersdorff et al., 2005; Koch et al., 1999; Yan and Cheng, 2006). This study investigates the expression pattern of the γ3 chain in mouse. We developed three new γ3-reactive antibodies, and we show that the γ3 chain is present in BMs. The distribution pattern is considerably more restricted than that of the γ1 chain and within any tissue there is differential deposition into BM compartments. This is particularly true in the retina and brain, where γ3 is uniquely expressed in a subset of the vascular basement membranes and the pial surface. We used conventional genetic ablation techniques to remove the γ3 chain in mice; unlike other laminin null mice (α5, β2, γ1 nulls) (Miner et al., 1998; Noakes et al., 1995; Smyth et al., 1999), these mice live a normal lifespan and have only minor abnormalities, the most striking of which are ectopic granule cells in the cerebellum and an apparent increase in capillary branching in the outer retina. These data support the suggestion that the γ3 chain is deposited in BMs and contributes some unique properties to their function, particularly in the nervous system.

[*]Corresponding Author: William J. Brunken, Professor and Director of Ophthalmic Research, Departments of Ophthalmology and Cell Biology, SUNY Downstate Medical Center, 450 Clarkson Ave, Box 5, Brooklyn, NY 11203, Voice 718-221-5328, Fax 718-270-3732, william.brunken@downstate.edu.
[#]Current Addresses: Yong Li, Harvard University Biological Labs, 16 Divinity Avenue, Cambridge, MA 02138

Keywords

Laminin; retina; CNS; cerebellum; angiogenesis; kidney; testis

1. Introduction

Laminins are heterotrimeric molecules composed of an α, a β, and a γ chain that function as key morphogens and regulatory elements (Colognato and Yurchenco, 2000; Yurchenco and Wadsworth, 2004). Genetic and developmental studies have revealed critical roles of laminins in mammalian morphogenesis. For example, deletion of the γ1 chain in mouse resulted in peri-implantation lethality in which the earliest basement membranes (BMs) underlying visceral and parietal endoderm failed to assemble (Smyth et al., 1999). Moreover, many human diseases have been related to defects in laminin chains including degenerative skin disorders (McGowan and Marinkovich, 2000), muscular dystrophies (Sunada et al., 1994) and eye abnormalities (Zenker et al., 2004).

At present, 5 α, 3 β and 3 γ chains are known in mouse and human (Aumailley et al., 2005). Of the currently fully described laminins, several contain the γ3 chain: α2β1γ3, α3β2γ3, α4β2γ3, α5β2γ3 and α3β3γ3 (Egles et al., 2006; Koch et al., 1999; Libby et al., 2000; Yan and Cheng, 2006). When the γ3 chain was first discovered, in addition to the canonical BM localization, it was found at epithelial apical surfaces including ciliated epithelial cells of lung, oviduct, epididymus, ductus deferens, and seminiferous tubules (Koch et al., 1999). More recently, the γ3 chain was shown to form a complex with integrin β1 at the apical surface of rat seminiferous epithelium and to regulate apical junction specialization (Siu and Cheng, 2004). However, recent data suggest that laminins containing the γ3 chain do not bind directly to integrins (Ido et al., 2008).

To further study the localization of the γ3 chain, we developed three new polyclonal antibodies using recombinant mouse γ3 chain short arm as the antigen. To study its functional role, we created a mouse lacking the expression of the γ3 chain (*Lamc3-/-*) by conventional homologous recombination. The specificity of the new antisera was confirmed by protein transfer blots from wild type and null tissues. These antibodies reacted with BMs in various tissues, indicating that the γ3 chain is broadly expressed. However, we observed distinct differences in the expression of the γ3 and γ1 chains. One clear difference is while γ1 is widely expressed in all vasculature, γ3 has restricted distribution to the vasculature of the brain and retina. Genetic deletion of *Lamc3* produced viable healthy mice with apparently normal lifespan and reproductive rates. The histogenic development of most tissues was largely normal. Two exceptions were the production of ectopic cells in the cerebellum and branching defects in the retinal vasculature.

2. Results

2.1 Generation and verification of Lamc3-/- mice and γ3 chain antibodies

Lamc3-/- mice were generated using a targeting vector designed to delete a 2.2kb fragment containing the entire first exon and part of the first intron of the *Lamc3* gene, inserting in its place a *LacZ* reporter gene and a neomycin resistance (*Neo*) cassette flanked by *LoxP* sites (Fig. 1A). Southern blot assays were used to confirm the genetic identity initially (Fig. 1B).

Three rabbit polyclonal γ3 chain antibodies, R40, R96 and R97, were produced by using recombinant mouse γ3 chain short arm as the antigen. To characterize these antibodies, we probed protein samples from testis of $Lamc3^{+/+}$ and $Lamc3^{-/-}$ mice. As additional controls, we used recombinant γ3 chain short arm (γ3SA) and EHS laminin. All three anti-short arm

antisera produced similar results (Fig. S1) and only those with R97 are shown (Fig. 1C). The reactivity of these three new anti-γ3 antisera is eliminated in Lamc3-/- mice. By contrast, while our previously produced antiserum, R16 (Koch et al., 1999) had γ3 specific reactivity, some immunoreactivity remained when it was reacted with tissue or protein samples from Lamc3-/- mice (Fig. S1). We, therefore, continued our analyses with the newly produced antisera.

Two bands were visualized in the wild-type sample ($\gamma3^{+/+}$); one migrated with an apparent mobility of 180kD and the other with a mobility of 120kD. The 120kD product is the predicted size of the γ3 short arm and the recombinant protein (γ3SA lane) has the identical mobility. The larger band corresponded to the full length γ3 chain (Iivanainen et al., 1999; Koch et al., 1999). Our interpretation is that γ3 chain is actively processed in the testis as it is in the placenta (Koch et al., 1999) as there are only two discrete products; if protein degradation was taking place, we would expect more random cleavage. Both knockout tissues ($\gamma3^{-/-}$) and EHS laminin (EHS) lanes are blank, demonstrating that there is no reactivity in these samples. Importantly, these data demonstrate that our antisera do not cross-react with the γ1 chain, which is a major component of EHS laminin. Immunohistochemistry using R96 confirmed the lack of protein production in the *Lamc3*$^{-/-}$ animals (Fig. 1D). In *Lamc3*$^{+/+}$ tissues, there was prominent labeling of BMs; there was no immunoreactivity (IR) in *Lamc3*$^{-/-}$ tissues.

2.2 The γ3 chain is differentially deposited in BMs

We used anti-γ3 antisera to study the distribution of the γ3 chain in various tissues, including somatic tissues and the central nervous system (CNS). In testis, γ3 IR was localized at the BM of seminiferous tubules (Fig. 2A). There was also weak γ3 IR in the interstitial space between tubules. Like the γ3 antibody, the perlecan antibody labeled the seminiferous tubular BMs heavily. In contrast to the γ3 antibody, the perlecan antibody heavily labeled vascular and other BMs in the interstitial space. These antisera demonstrated no obvious γ3 IR at the apical surface in seminiferous tubules, similar to the results reported by others (Siu and Cheng, 2004). In kidney, the γ3 IR was present largely in Bowman's capsule and mesangium, and weakly in glomerular BM (GBM), as well as somewhat weakly and discontinuously in tubular BM (Fig. 2B, 7). By contrast, perlecan IR was evenly distributed in the GBM and in the BMs of kidney tubules (Fig. 2E). The γ3 IR was present in the dermal BM and around the hair follicle and was particularly strong at the lower part of the follicular BM continuing around the hair papilla (Fig. 2C). The staining at the dermal border, is similar to that previously reported (Koch et al, 1999). In contrast, perlecan is more evenly and more broadly distributed in all BMs of the skin (Fig. 2F). Thus, we conclude that the γ3 chain is incorporated into laminins that are not deposited in all BMs but rather have restricted expression in some compartments even within a single tissue, suggesting that the γ3-containing laminins may have specific roles in these locations.

2.3 The γ3 chain is expressed widely in the CNS

Because three laminins containing the γ3 chain have been isolated from the central nervous system (Egles et al., 2006; Libby et al., 2000), we studied the expression of the γ3 chain in detail in the CNS, starting with the retina (Fig. 3). In the adult retina, there are three BMs: Bruch's membrane, the inner limiting membrane (ILM) and vascular BM (Libby et al., 2000). All these BMs were immunoreactive for perlecan. However, γ3 IR is present in Bruch's membrane, is very clearly in the intra-retinal vascular BM and is weakly detectable in the ILM (Fig. 3A). The ILM is lightly reactive for γ3 in most regions (Fig. 3C) except at the attachment site of the vitreous body near the head of the optic nerve.

Most surprisingly, we found γ3 antibodies react with intracellular stores in cells of the inner nuclear layer (INL) (Fig. 3A). Paraformaldehyde (PFA) fixation of the retina greatly reduced the apparent γ3 IR in BMs, presumably by epitope masking. However, the intracellular γ3 IR persisted and allowed us to identify the cells as a subset of retinal neurons. We double-labeled the PFA-fixed retina with γ3 antibody and antibodies against several cell markers including calretinin, calbindin, glutamine synthetase (GS) and vesicular glutamate transporter 3 (VGLUT3) (Figs. 3B, S2). Calretinin labels many different types of amacrine cells, displaced amacrine cells and possibly all ganglion cells; calbindin labels horizontal cells; GS labels exclusively Müller cells (Haverkamp and Wassle, 2000). VGLUT3 is expressed by a subset of amacrine cells (Johnson et al., 2004). Although several cell types contain γ3 IR, the only cell type that we could unequivocally demonstrate as containing γ3 IR was the VGLUT3 expressing amacrine cell; all VGLUT3 cells were labeled with the γ3 antibody (Fig. 3B). Calretinin and calbindin expressing cells were γ3 IR negative (Fig. S2). It is noteworthy that there was no intracellular accumulation of γ3 in Müller cells (GS+) (Fig. S2), despite prior in situ hybridization studies that demonstrated transcripts in Müller cells (Libby et al., 2000). The accumulation of γ3 in intracellular stores in VGLUT3 amacrine cells is reminiscent of experiments using gene trap techniques (Yin et al., 2003). It suggests perhaps a lack of suitable laminin chain partners required for secretion. Nevertheless, these data suggest that both neurons and glia may be sources of laminins.

Laminin expression is regulated both spatially (in tissue distribution) and temporally (during development). Thus, we examined the spatial and temporal expression of the γ3 chain along with the two other γ chains during development (Fig. 3C). In general, γ3 chain expression is delayed and spatially more restricted than that for the γ1 chain; the γ2 chain is not expressed in the neural retina (Fig. 3C). From E13, the earliest time point that we examined, γ3 IR is found associated with the choriocapillaris, hyaloid vessels and Bruch's membrane. At this point in development, the γ1 chain is heavily expressed in these same BMs, in the lens capsule (BM of the lens) and indeed in the vitreous body. Weak, but reproducible, γ2 IR is present on both sides of the RPE (subretinal space) and in Bruch's membrane, as well as in the lens capsule. Importantly, no γ3 IR is detectable in the optic nerve except in the dural BM, whereas the γ1 chain is well expressed in the optic nerve, both in the dural BM and in the basal lamina of optic nerve fibers themselves.

2.4 The γ3 chain is a widespread component of CNS vasculature

Because of its geometric organization, retinal vasculature is particularly amenable to study; thus we concentrated our studies on the deposition of γ3 chain in retinal vascular BM during development. Retinal vasculature develops in humans around mid-gestation and in mice largely after birth (Connolly et al., 1988). Moreover, there are three layers of retinal vessels: superficial vessels at the vitreal border, penetrating vessels, with capillary expansion in the INL; and deep capillary plexus in the outer plexiform layer (OPL) (Fig 3A; perlecan or Fig 10 A,C,E,G). Concomitant with retinal vascularization, γ3 chain deposition is up-regulated. Particularly striking is the association with the central vessels (Fig. 3C, P7, arrow). The association with retinal vasculature continues and is maintained in the adult retina; the γ3 chain is heavily expressed in the microvasculature (Fig. 3A) and in some medium caliber vessels at the retinal vitreal surface.

In order to further understand the distribution of γ chains in the retinal vasculature, we studied their distribution in retinal whole-mounts, which allow complete visualization of the vascular tree throughout their penetration of the retina. The distribution of γ1 and γ3 chains in the retinal vasculature is shown in Figure 4; there was no γ2 IR detectable in blood vessels (data not shown). The γ1 chain is widely expressed over the whole retinal vascular architecture including both the arteries and the veins at the vitreal surface (Fig. 4A). In

contrast, the spatial distribution of the γ3 chain is more restricted (Fig. 4B); γ3 IR is not seen in the arteries, but is in the veins at the vitreal surface of the retina (Fig. 4C). Deeper in the retina, γ3 chain IR is also present in the small diameter arterioles located in the INL (Fig. 4D) also visible here are various neurons expressing the molecule. The deepest capillary bed found in the OPL (Fig. 4E) is strongly reactive. This distribution of γ3 chain IR at the vitreal surface, arterioles and capillary bed is also demonstrated in cross-sections of retinae (Fig. 7, below). Thus, while the two γ chains overlap in distribution, the γ3 chain appears to discriminate between arteries and veins.

We also examined the expression of the γ3 chain in the brain. γ3 IR is seen at the pial BM in all regions of the P6 brain (Fig. 5A) as well as some portions of vascular BMs. We presume that, based our retina studies, these are veins and small diameter capillaries. In contrast to the limited distribution of the γ3 chain, the γ1 chain is relatively evenly distributed along the pial BM and throughout the vascular BM (Fig. 5A).

We examined the developmental expression of the γ chains (Fig. 5B). We were particularly interested in the expression pattern in the cerebellum. Several generalizations can be made: the γ2 chain is not heavily expressed in the cerebellum; γ3 chain expression temporally lags that of the γ1 chain and is spatially more restricted (Fig. 5B). At E11, the γ3 chain is expressed only in the meningeal compartment, particularly the pial surface. As the cerebellar anlage expands, γ3 expression is maintained in the pial BM and begins to be expressed in the vascular supply. At E13, the γ1 chain is well expressed in the brain vasculature, as well as in the meninges; diffuse γ1 IR is also present in the cerebellar ventricular zone (Fig. 5B, γ1, E13, arrow). The γ1 IR in the cerebellar vasculature is robust throughout development, suggesting that the γ1 chain is expressed at all levels of the vasculature, as it is in the retina. In contrast, the γ3 IR has a more limited spatial distribution than the γ1 IR. Both γ1 and γ3 IR are seen in the choroid plexus throughout cerebellar development (Fig 5B, arrowheads).

Remarkably, γ3 IR is largely absent in vasculature outside the CNS. For example, although γ3 IR is prevalent in the BM of the hair follicles and basement membrane of the skin, it is absent from the PECAM-expressing vasculature of the skin (Fig. 6). Thus, unlike the γ1 chain, the γ3 chain is a component of the CNS vasculature, but not of peripheral vessels.

2.5 Compensation by other γ chains in the Lamc3$^{-/-}$ mouse

How does removal of the γ3 chain affect the expression of the other γ chains; i.e., is there any compensation by either the γ1 or the γ2 chain in the *Lamc3*$^{-/-}$ mice? To address this question, we first compared γ chain expression by immuno-histochemistry in several tissues (Fig. 7). γ3 IR disappears in the *Lamc3*$^{-/-}$ testis, kidney, skin and retina. Because the γ2 chain has unique structural organization, and appears to partner exclusively with the β3 chain, we did not expect any compensation by this chain in the *Lamc3*$^{-/-}$ tissues. Indeed, there is no obvious change in the γ2 chain expression in the mutant animal. Immunohistochemical distributions of γ1 chain did not change significantly in the *Lamc3*$^{-/-}$ animal (Fig. 7).

To correlate that there was also no change in γ1 chain transcription upon removal of the γ3 chain, we compared γ1 chain mRNA levels in the retina and testis of the *Lamc3*$^{-/-}$ and *Lamc3*$^{+/+}$ littermate animals. We measured mRNA by quantitative PCR (QPCR) (Table 1). The γ1 mRNA levels were judged by the ΔCt method (details in Methods) using 18S ribosomal RNA as the control reference. For retina, the ΔCt was 15.5 ± 1.8 (n=7) in the wild-type and was 15.4 ±1.0 (n=9) in the mutant; for testis, the numbers were 11.9 ± 0.5 (n=2) and 12.3 ± 0.3 (n=3) respectively. Thus, in neither tissue was there a significant difference in transcription between the *Lamc3*$^{+/+}$ and the *Lamc3*$^{-/-}$ animals, consistent with the lack of significant changes in immunohistochemical distribution.

2.6 Somatic tissue phenotype of the Lamc3$^{-/-}$ mouse

Given there is little change in expression of the γ1 or γ2 chain, how does the removal of the γ3 chain affect tissue morphology and function? The *Lamc3*$^{-/-}$ mice survive into adulthood; they are able to breed and have similar body size with their heterozygous and wild type littermates. In kidney, testis, and fallopian tube, where the γ3 chain is richly expressed in the wild type animals (Koch et al., 1999), tissue organization in the *Lamc3*$^{-/-}$ animals has normal polarity and compartmentalization (Fig. S3). One subtle difference is that the parenchyma/stroma ratio appears altered. Specifically, the epithelial packing density appears looser, with increased interstitial space between the tubules in kidney and testis; the stomach crypts are of shorter length and less complexly branched. It is possible that such subtle defects are the result of tissue processing, but they have been consistently observed, and it may well be that the matrix of the *Lamc3*$^{-/-}$ animals is less resilient than that of the wild type animals.

Because the γ3 chain is richly expressed in hair follicles of the skin (see Figs. 2C, 5A), removal of the γ3 chain may affect hair development. We prepared skin samples from the backs of *Lamc3*$^{-/-}$ mice and their *Lamc3*$^{+/+}$ littermates. We did not observe a significant change in hair follicles in the *Lamc3*$^{-/-}$ compared to the *Lamc3*$^{+/+}$ skin (data not shown).

2.7 Retinal phenotype caused by the γ3 chain deletion is limited to the vasculature

Because laminin β2 chain deletion disrupts retinal architecture and function (Libby et al., 1999), we examined how γ3 chain deletion would affect retinal architecture and function (Fig. 8). Retinal lamination, thickness and basic organization were unchanged. In contrast to the dysmorphic photoreceptor layer in the *Lamb2*$^{-/-}$ retina (Libby et al., 1999; Pinzon-Duarte et al., 2010), the expression of two photoreceptor markers, recoverin and rhodopsin, and the thickness of both the outer nuclear layer (ONL) and the outer segment were all normal in the *Lamc3*$^{-/-}$ retina (Fig. 8A). Calretinin was detectable in a variety of amacrine cells with typical tri-laminate processes in the inner plexiform layer (IPL) and many cells in the ganglion cell layer in the *Lamc3*$^{+/+}$ retina (Fig. 8A, upper row); there was no readily apparent change in this organization in the *Lamc3*$^{-/-}$ retina (Fig. 8A, lower row). Müller cells, containing GS, maintained normal radial orientation of their processes as well as normal architecture of their end-feet at both the external limiting membrane (ELM) and the ILM. No elevation of GFAP was apparent in the mutant, indicating that Müller cells are not in reactive gliosis. To evaluate the function of the retina, electroretinograms (ERGs) were carried out on *Lamc3*$^{-/-}$ mice and their *Lamc3*$^{+/+}$ littermates. The ERG consists of an a-wave, the summed potential from photoreceptors, and a b-wave, the summed potential from second order cells. No large changes in ERGs were obtained in either the a- or the b-wave (Fig. 8B), although the b-wave may be somewhat reduced in the *Lamc3*$^{-/-}$ mice. These data suggest that the transduction and synaptic transmission between photoreceptor and second order neurons is not greatly affected by the γ3 chain removal from the retina.

Given the distribution of the γ3 chain in the optic nerve head and the role of laminin α1β1γ1 (laminin 111) in intraretinal axon guidance, we assayed if there were changes in ganglion cell targeting to the optic nerve in the *Lamc3*$^{-/-}$ animals. We labeled all retinal ganglion cells (RGCs) with TuJ-1, an antibody to neurotubulin, in retina whole-mounts. In both the *Lamc3*$^{-/-}$ and the *Lamc3*$^{+/+}$ retinas, RGC axons collect into fascicles that run without errors to the optic nerve head (Fig. 9).

Because there is a specific association of the γ3 chain with the retinal microvasculature, we determined whether there was a change in retinal vascularization in *Lamc3*$^{-/-}$ animals. No signs of bleeding were seen in the retina or brain of the *Lamc3*$^{-/-}$ animals. However, there was a minor increase in the capillary density in the retina. We stained retina whole-mounts with antibodies to PECAM (CD31) to assay the retinal vasculature (Fig. 10). We assayed all

three levels of retinal vasculature, those at the vitreal surface, and the intermediary (INL/IPL) and deep (OPL) plexuses. Removal of the γ3 chain does not disrupt the distribution of retinal vessels on the surface of the retina (Fig. 10A, B) as the entire retina is vascularized. Nor is the branching pattern of the larger arterial supply affected by the mutation (Fig. 10C, D). However, slight increases in the branching of the deep (OPL) capillary bed and more frequent anastomoses were noted (Figs. 10E, F; 10G, H).

2.8 Ectopic cells in the Lamc3$^{-/-}$ cerebellum

Based on the γ3 chain expression data in mouse cerebellum (Fig. 5B), we asked whether there were any defects in the *Lamc3*$^{-/-}$ cerebellum. After birth, cerebellar granule cells are generated by granule cell precursors (GCPs) in the external germinal layer (EGL) and then migrate from the EGL inwardly along Bergmann cell processes to form the internal granule cell layer (IGL); by P21, all the granule cells have migrated into the IGL and no granule cells are left in the EGL (Goldowitz and Hamre, 1998).

We compared the cerebella of *Lamc3*$^{-/-}$ and *Lamc3*$^{+/+}$ animals at P30 (Fig. 11). The anterobasal and central lobes (Fig 10, A and C, boxed) of the *Lamc3*$^{-/-}$ cerebellum appear to have more convolutions than those of the *Lamc3*$^{+/+}$ cerebellum; the anterodorsal, the posterior and the inferior lobes look similar in the *Lamc3*$^{-/-}$ and the *Lamc3*$^{+/+}$ cerebella. More dramatically, ectopic cells are present at the pial surface of the cerebellum between the folia (Fig. 11D, white arrow) and within the molecular layer (ML) (Fig. 11D, black arrows) of the *Lamc3*$^{-/-}$ cerebellum. Because granule cells develop at the pial surface, and then migrate into and through the molecular layer and past the Purkinje cell layer, we interpret these findings as a reduction of the success rate for granule cell migration. No disruption in the organization of the Purkinje cell layer was detectable.

Discussion

Summary of the principal findings

Previous studies from several laboratories including our own have suggested that the laminin γ3 chain is expressed on both the basal and the apical sides of various epithelial tissues as well as the neural retina (Koch et al., 1999; Libby et al., 2000; Yan and Cheng, 2006); in contrast, one report suggested that the γ3 chain was exclusively expressed in the BMs (Gersdorff et al., 2005). We produced three new γ3 chain antisera and tested them against *Lamc3-/-* mouse tissues for specificity. The reactivity of all three antisera was abolished by transgenic ablation of the *Lamc3* gene. Using these antibodies, we demonstrated that the γ3 chain was deposited in the BMs of various tissues including kidney, testicular tubules, skin and its appendages, the CNS, and the vascular system. However, the γ3 chain is more restricted in distribution when compared to the γ1 chain or perlecan, which are distributed uniformly in all BMs (Iozzo et al., 1994; Smyth et al., 1999). γ3 expression in skin is restricted to the papillae and distal portions of hair follicles and discrete regions of the dermal-epidermal junction, and γ3 is absent from the vasculature of the skin. The kidney also shows compartmental localization of the γ3 chain, with the γ3 chain largely limited to basement membranes of Bowman's capsule and tubules. However, the most dramatic example of the spatial restriction of the γ3 chain expression was found in the retinal blood supply, where the γ3 chain is restricted to small arterioles, capillaries and veins. No γ3 chain deposition was found in arterial BMs.

Some neurons express the γ3 chain

The identification of a neuronal source of laminins in the CNS remains somewhat controversial. However, there is growing evidence that neurons can be a cellular source of laminins (Egles et al., 2006; Liesi et al., 2001). Our data show that some retinal amacrine

cells display γ3 IR (Fig. 2B). The identity of the amacrine subtype that expresses γ3 is not known with certainty. We can exclude those multiple classes of amacrine cells expressing calretinin, while we can include the subset of VGLUT3+ amacrine cells. The cellular labeling of amacrine cells is unlikely an artifact, because all neuronal γ3 IR disappears in the *Lamc3-/-* retina. Because laminins are expressed as heterotrimers, γ3 chain synthesis and release necessarily requires the expression of other laminin chains; we do not have any information on other laminin chains being expressed by the γ3+/VGLUT3+ amacrine cells. However, it seems reasonable that neuron secretion of laminins is possible as others have demonstrated the presence of laminin chains (β1 and γ1) in CNS neurons, including in the retina, using gene trap methods (Yin et al., 2003). In addition, data from both the peripheral and central nervous systems support the hypothesis that target-derived laminin is important for synapse stabilization (Egles et al., 2006). While we have detected expression of laminin α chains in cortical and cerebellar neurons (Brunken, unpublished data), they have not been reported in the retinal neurons. Thus, whether neurons synthesize and secrete laminins in the CNS remains an unanswered question.

Compensation by other γ chains in Lamc3-/- mice

Laminins are a key component in BMs and are essential for BM assembly (Yurchenco and Wadsworth, 2004). Minor defects are observed in many somatic tissues of the *Lamc3-/-* mouse, such as skin, testis, and kidney. In none of these tissues is there a disruption of the fundamental organization of the BM. Moreover, the reproductive function of the *Lamc3-/-* animals is not changed, indicating no profound disruptions in embryonic implantation or development such as that that occurs with mutations in the *Lamc1* gene. These are indirect observations, however. Direct ultrastructural and immunochemical analysis of the two BMs of the retina showed that there was no change in the *Lamc3-/-* mouse (Pinzon-Duarte et al, 2010). Given that the γ1 and γ3 chains share considerable identity in their primary sequences, it is reasonable to suggest that the γ1 chain can substitute for the γ3 chain. The expression studies above certainly support this suggestion insofar as the γ1 chain is expressed earlier than the γ3 chain and has a broader distribution than the γ3 chain. However, the existence of at least two defects in the *Lamc3-/-* mouse (cerebellar and vascular phenotypes) clearly demonstrates that the γ1 chain cannot fully compensate for the γ3 chain.

γ3 chain in vasculature: A new avenue to study retinal vasculogenesis

Laminin expression in vascular BMs of somatic tissues and the CNS, including the retina and the brain, are regulated both spatially and temporally. For example, two laminin isoforms, α4β1γ1 and α5β1γ1, were found in the CNS vascular BM; α4β1γ1 is expressed by all endothelial cells regardless of the stage of development while α5β1γ1 is found only at capillaries and venules starting at P21 (Hallmann et al., 2005). In this study, we observed differential distribution of the γ3 chain in the BMs of the CNS vessels and not in blood vessels outside of the brain or retina. In the retina, where the vascular tree can be displayed as a sheet, it was clear γ3 was deposited in the micro-vascular and venous BMs, whereas the γ1 chain is distributed homogeneously. RT-PCR studies of various tissues, demonstrate that γ3 is not ubiquitously expressed, as it would were it expressed in all blood vessels (Koch et al, 1999). In contrast, it has been long appreciated that the β2 chain is widely expressed in the vascular system and spatially segregated (Sanes et al., 1990). Similarly, using retina whole-mounts, we have shown that the β2 chain is expressed over most of the vascular tree but is more heavily expressed in arteries than veins (Brunken, unpublished observations). Together with data from other laboratories (Fujita et al., 2005; Sorokin et al., 1994; Sorokin et al., 1997), several laminins have been suggested to be expressed in the CNS vasculature: α4β1γ1, α5β1γ1, α4β1γ3, α5β1γ3, α4β2γ3, and α5β2γ3. All of these laminins have been isolated from various tissues with the exception of α5β1γ3, which would necessarily be

expressed only in the capillary and venous BM. It is interesting to note that two of these laminins, α5β2γ3 and α4β2γ3, were isolated from the retina (Libby et al., 2000).

Given the restrictive γ3 chain expression in the vascular BM of the CNS, several questions arise: what is the function of the γ3 chain-containing laminins in the CNS vasculature; what is the γ3 chain cell source in the vasculature; how is the γ3 chain developmentally regulated; is the restrictive γ3 deposition causally linked to the arterial-venous boundary? The increased branching of the capillary bed observed in the *Lamc3-/-* mouse suggests indeed that these laminins are regulating an important aspect of vasculogenesis – capillary branching patterns. No shifts in the arterial and venous patterning in the retina were seen in the *Lamc3-/-* mouse. A complete study of the role of *Lamc3* and *Lamb2* in retinal angiogenesis is underway and demonstrates that *Lamc3* has a developmentally delayed angiogenesis (Gnanaguru and Brunken, unpublished data).

Studies on laminin α chains also point to the regulation of vascular development by laminins: the *Lama4-/-* mouse has a bleeding phenotype, resulting from a disruption of the microcirculation (Thyboll et al., 2002); the *Lama5-/-* mouse has vascular dysgenesis and defective glomerulogenesis, both of which are at the level of the microvasculature (Miner and Li, 2000). However, the mechanism of laminin regulation is not yet known. The distribution of integrins and other laminin receptors on retinal vasculature is not fully reported; nor is there much information available on the developmental regulation of the laminin isoforms. Further experimentation is warranted.

Lamc3-/- cerebellum and integrin β1 conditional knockout mouse cerebellum

The γ3 chain is expressed in the pial BM throughout cerebellar development. Moreover, after targeted ablation of the *Lamc3* gene, ectopic granule cells appear in the *Lamc3-/-* cerebellum. Many defects affecting Bergmann glia adhesion to the pial BM have been found to result in ectopic granule cells. In the mouse mutant of Jagged1, a ligand for the Notch family receptors, Bergmann glia lost contact with the pial surface and ectopic granule cells were observed (Weller et al., 2006). In the integrin β1 conditional knockout (Itgb1 CKO) mouse cerebellum, Bergmann glia failed to reach the pial BM, so that ectopic granule cells resulted (Graus-Porta et al., 2001). Therefore, the ectopic cells in the *Lamc3-/-* cerebellum may be due to Bergmann glia defects. Further examination of Bergmann glia in the *Lamc3-/-* mice should be performed. Besides the ectopic cells, abnormal foliation in the anterobasal and central lobes was also observed in the *Lamc3-/-* cerebellum. Interestingly, the Itgb1 CKO cerebellum had a similar but more severe foliation pattern in the anterobasal and central lobes (Blaess et al., 2004; Graus-Porta et al., 2001). The conditional knockout mouse of integrin-linked kinase (ILK), a downstream protein in the integrin signaling pathway, also showed a similar foliation abnormality as the *Lamc3-/-* (Belvindrah et al., 2006; Mills et al., 2006). Therefore, it seems reasonable to suggest that γ3-containing laminins contribute to granule cell migration either directly or by stabilizing interactions with the Bergman glial cell.

These disruptions in cerebellar anatomy are interesting and along with our other work in retina (Pinzon-Duarte et al, 2010 and Denes et al 2007), suggest that γ3-containing laminins are important in CNS development and function. Importantly, recent reports have linked mutations in the LAMC3 gene to human disease including autism and congenital malformation of the occipital lobe along with diminished mental capacity (O'Rouk et al., 2011; Barak et al 2011).

Experimental Procedures

Mice

All procedures involving animals were approved by Tufts and Downstate Animal Care and Use Committees (IACUC) and were in accordance with the National Institute of Health Guide for the Care and Use of Animals, and the policies of the Society for Neuroscience and the Association for Research in Vision and Ophthalmology.

Lamc3-/- mice were generated using standard recombination methods. A mouse 129/SvJ genomic DNA BAC library (Genome Systems, St. Louis, MO) was screened by PCR using primers derived from exon 2 of the human *Lamc3* gene (MF155 – GCTTATGAGATCACGTATGTGAG and MF128 – CTGCAGCCCAGGGCTCTCCTCGAA). The BAC clone insert was shotgun-subcloned after restriction endonuclease digestion. The resulting library was screened for plasmids containing inserts from the 5′ end of the *Lamc3* gene. The targeting construct was created by cloning a 3.6kb BamHI fragment containing the promoter and the 5′ UTR of the *Lamc3* gene together with the SalI fragment of pGT1.8 Ires βgeo (Mountford et al., 1994) and a 4.3kb EcoRV-KpnI fragment of intron 1 of the *Lamc3* gene. The resulting targeting vector created a 2.2kb deletion spanning exon 1 and part of intron 1 of the *Lamc3* gene and replaced it with a promoter-less IRES β-Geo cassette. The targeting construct was linearized and electroporated into 129/SvJ ES cells. Neomycin-resistant ES cell clones were selected and expanded. Genomic DNA was extracted from these ES cells for Southern blotting. The DNA was digested with HindIII alone or HindIII plus EcoRI, and then probed with external 5′ and 3′ probes. The 5′ probe detects a 10.5kb HindIII fragment from a wild type allele and a 5.9kb fragment from a correctly targeted recombinant allele. The 3′ probe detects an 8.0kb HindIII/EcoRI fragment from a wild-type allele and a 6.7kb fragment from a recombinant allele. Selected ES cells were then injected into C57BL/6 blastocysts. Genome Systems, Inc., St. Louis, MO created the targeting construct and generated germ line transmitting chimeric mice. Heterozygous mice were mated to generate homozygous null mice. The *Neo* cassette was removed by mating the heterozygous mouse with a sperm-*Cre*-expressing mouse (Lewandoski et al., 1997). Heterozygous mice were mated and genotypes of their offspring were determined by PCR analysis of the genomic DNA prepared from tail or toe samples. Primers used: wild type allele, forward GTGAAAGGATGGATGGATGG, reverse CCCCAATCTGAGCACCTGTA; null allele, forward TTCCTGAGGCCGATACTGTC, reverse CACCACATACAGGCCGTAGC.

Recombinant expression and purification of mouse γ3 fragment

Mouse γ3 chain short arm (AF079520, nucleotides 1 - 3122) was expressed and purified similarly as previously described (Koch et al., 2000).

Antibody production

Three rabbit polyclonal γ3 antibodies, R40, R96 and R97, were produced as described previously (Libby et al., 2000). Briefly, purified recombinant γ3 chain short arm was injected intradermally into a rabbit following standard procedures (Harlow and Lane, 1988). The R40, R96 and R97 antisera were loaded over a protein G column (Amersham Biosciences, Piscataway, NJ), eluted with triethylamine (Sigma, St. Louis, MO) and neutralized. The neutralized eluate was affinity-purified through an activated CNBr-Sepharose column (Amersham Biosciences) to which the recombinant mouse γ3 chain short arm had been coupled after the cleavage of its His tag. Bound antibodies were eluted with triethylamine at pH 11.5. The elution was immediately neutralized and dialyzed against phosphate buffered saline (PBS).

Immunohistochemistry

For fresh-frozen samples, adult or embryonic tissues were embedded immediately in OCT compound (Sakura, Torrance, CA) and frozen by immersion in dry ice-cooled ethanol. For fixed tissues, mice were anesthetized by intramuscular injection of ketamine and xylamine, and then transcardially perfused by PBS followed by 4% paraformaldhyde (PFA) in PBS. After further fixation in 4% PFA by immersion, tissues went through 10%, 20% and 30% sucrose before embedded in OCT. For both fresh-frozen and 4% PFA fixed tissues, 12 μm thick sections were cut with a Reichert-Jung 2800 Frigocut cryostat and placed onto Superfrost Plus slides (Brain Research Laboratory, Newton, MA). Slides were stored at -80°C until use. Upon use, slides were returned to room temperature and air-dried. Fresh-frozen tissue slides were immersed in methanol at -20°C for 2 minutes; 4% PFA-fixed tissue slides directly went to the next step. Slides were then washed in PBS, and blocked with 1% BSA and 5% goat or donkey serum in PBS for 1 hour. Slides were then incubated in primary antibody for 2 hours at room temperature or overnight at 4°C. Antibodies used: R40 (1:5,000), R96 (1:10,000) and R97 (1:10,000), laminin γ1 chain antibody 1083 (rabbit polyclonal from the late Dr. Rupert Timpl; 1:5,000) (Schymeinsky et al., 2002), laminin γ2 chain antibody (rabbit polyclonal, 1:5,000) (Sugiyama et al., 1995), perlecan (rat monoclonal, 1:50,000; Chemicon, Temecula, CA), calretinin (mouse monoclonal, 1:1,000; Chemicon), calbindin (mouse monoclonal, 1:500; Sigma), VGLUT3 (rat monoclonal, 1:500; Chemicon), glutamine synthetase (mouse monoclonal, 1:1,000; Chemicon), PECAM (CD31) (rat monoclonal, 1:1,000; Chemicon), GFAP (rabbit polyclonal, 1:5,000; Chemicon), recoverin (mouse monoclonal, 1:1,000; Chemicon), and rhodopsin (mouse monoclonal, 1:10,000; Sigma).

Primary antibodies were diluted in 1% BSA and 1% goat or donkey serum in PBS. After a PBS wash, slides were incubated in species-appropriate, affinity-purified, fluorescently labeled secondary antibodies (Invitrogen, Carlsbad, CA) for 1 hour at room temperature. Some slides were counter-stained with DAPI (Sigma). After a PBS wash, slides were mounted in Prolong or Prolong-Gold (Invitrogen) to reduce photobleaching. Slides were examined with a Nikon E800 microscope (Nikon Instruments, Melville, NY). Images were captured using Openlab 4.0.2 software (Improvision Inc., Lexington, MA) with an Orca-ER camera (Hamamatsu, Bridgewater, NJ). Figures were created in Adobe Photoshop 7.0 (Adobe Systems, San Jose, CA) and no enhancements other than contrast and brightness were made. For montage images, series of images were taken using Openlab 4.0.2 with a motorized X-Y stage. After background subtraction, individual images were assembled into a montage with GraphicConverter software (Lemke Software GmbH, Peine, Germany).

Immunohistochemistry on retina whole-mounts

Retina whole-mounts were prepared similarly as previously described (Cellerino et al., 1998). Mice were anesthetized by intramuscular injection of ketamine and xylamine, and then transcardially perfused by PBS followed by 4% PFA in PBS. The eyes were enucleated and the anterior segment was removed and discarded. Eyecups were further fixed in 4% PFA in PBS for 30 minutes. Retinas were dissected out and four radial cuts were made to allow flattening. The retinas were dehydrated in ascending ethanol concentrations (50%, 70%, 80%, 90%, 95%, and 100%) for 10 minutes each, then defatted in xylene for 10 minutes, and then rehydrated in a descending ethanol series for 10 minutes each. After a PBS wash, retinas were blocked with 1% BSA in PBS with 20% goat or donkey serum and 0.3% Triton X-100 overnight at 4°C; then incubated in primary antibodies in 1% BSA in PBS with 5% goat or donkey serum for 3 days at 4°C with continuous agitation. Primary antibodies used were R96 (1:5,000), 1083 (1:5,000), and anti-neurotubulin (TuJ-1, mouse monoclonal, 1:500; Covance Innovative, Berkeley, CA). After a PBS wash, retinas were incubated in species-appropriate, affinity-purified, fluorescently labeled secondary

antibodies for 1 day at 4°C in the same buffer with continuous agitation. After a PBS wash, retinas were flattened on slides with the ganglion cell layer facing upward and covered with Prolong or Prolong-Gold (Invitrogen). The slides were stored at 4°C between examinations.

Protein transfer blots

Protein transfer blots and sample preparation were performed as previously described (Libby et al., 1997). Tissues were removed from mice and were used immediately or stored at -80°C. For extracellular matrix protein extraction, tissues were sonicated in 1 ml lysis buffer (25 mM Tris, 0.2 mg/ml α2-macroglobulin, pH 7.5) per 50 mg of tissue for 30 seconds on ice. Homogenates were then centrifuged at 15,000 × g for 10 minutes at 4°C. The supernatants, containing the cytosol, were disposed. The pellets, containing the extracellular matrix, were resuspended in 250 μl 5 × sample buffer [50% (vol/vol) glycerol, 36% (vol/vol) β-mercaptoethanol, 15% (wt/vol) sodium dodecylsulfate (SDS), 630 mM Tris, pH 6.8] per 50 mg of the original tissue.

10 μl of each protein sample was resolved by 5% polyacrylamide-SDS gels (SDS-PAGE) and then electro-transferred to PVDF membranes (Bio-Rad, Hercules, CA). Blots were blocked with 5% non-fat milk (Bio-Rad) in PBS-T (PBS with 0.05% Tween-20) and then incubated overnight at 4°C with primary antibodies diluted in 1% non-fat milk in PBS-T. The primary antibodies used were: R40, 1:50,000; R96, 1:100,000; R97, 1:100,000. The blots were washed and incubated for 1 hour at ambient temperature with horseradish peroxidase-conjugated secondary antibodies (1:10,000; Chemicon, Temecula, CA). Chemiluminescent detection was performed by using the Western Lightening Chemiluminescence Reagent Plus kit (PerkinElmer, Boston, MA) and documented on X-Omat Blue films (Kodak, Rochester, NY).

Histology

P30 mice were anesthetized by intramuscular injection of ketamine and xylamine and then transcardially perfused with PBS followed by 4% PFA in PBS. Various tissues were dissected and further fixed in 4% PFA in PBS by immersion overnight at 4°C. Then they were transferred to 70% ethanol until they were processed for paraffin embedding. 5 μm thick sections were cut with a Leica RM2265 microtome (Leica Microsystems, Bannockburn, IL). Every 10th section was collected and stained using a Haematoxylin and Eosin protocol.

Reverse transcription- (RT-PCR) and quantitative-polymerase chain reaction (QPCR)

Total RNA was isolated from P30 mice using Trizol (TRIzol LS Reagent, Invitrogen)/ Chloroform per the manufacturer's recommendation. RNA samples were treated with DNase I (Ambion, Austin, TX) per the manufacturer's recommendations to destroy any DNA contaminates and then reverse-transcribed using a SuperScript II First-Strand Synthesis System for RT-PCR (Invitrogen) primed with random hexamers per the manufacturer's recommendations. The obtained cDNA samples were used for QPCR. QuantiTect SYBR Green Kits (Qiagen, Valencia, CA) were used for the QPCR. About 200 pg cDNA was used as template for each reaction. A 501bp fragment at γ1 Domain III was amplified with a forward ACGGCTACTTTGGAGACCCT primer and reverse GTCCAAACCCAAAGTGGTTG primer. A dilution series of one sample was used to create a standard curve. The reactions were performed in triplicate in an Mx4000 Multiplex Quantitative PCR System (Stratagene, La Jolla, CA).

Supplementary Material

Refer to Web version on PubMed Central for supplementary material.

Acknowledgments

Supported by Grants: NS 39502 (REB,WJB) and EY 12767 (WJB)

References

Aisenbrey S, Zhang M, Bacher D, Yee J, Brunken WJ, Hunter DD. Retinal pigment epithelial cells synthesize laminins, including laminin 5, and adhere to them through alpha3- and alpha6-containing integrins. Invest Ophthalmol Vis Sci. 2006; 47:5537–44. [PubMed: 17122146]

Aumailley M, Bruckner-Tuderman L, Carter WG, Deutzmann R, Edgar D, Ekblom P, Engel J, Engvall E, Hohenester E, Jones JC, Kleinman HK, Marinkovich MP, Martin GR, Mayer U, Meneguzzi G, Miner JH, Miyazaki K, Patarroyo M, Paulsson M, Quaranta V, Sanes JR, Sasaki T, Sekiguchi K, Sorokin LM, Talts JF, Tryggvason K, Uitto J, Virtanen I, von der Mark K, Wewer UM, Yamada Y, Yurchenco PD. A simplified laminin nomenclature. Matrix Biol. 2005; 24:326–32. [PubMed: 15979864]

Barak T, Kwan KY, Louvi A, Demirbilek V, Saygı S, Tüysüz B, Choi M, Boyacı H, Doerschner K, Zhu Y, Kaymakçalan H, Yılmaz S, Bakırcıoğlu M, Çağlayan AO, Öztürk AK, Yasuno K, Brunken WJ, Atalar E, Yalçınkaya C, Dinçer A, Bronen RA, Mane S, Özçelik T, Lifton RP, Šestan N, Bilgüvar K, Günel M. Recessive LAMC3 mutations cause malformations of occipital cortical development. Nature Genetics. 2011; 43:590–594. [PubMed: 21572413]

Belkin AM, Stepp MA. Integrins as receptors for laminins. Microsc Res Tech. 2000; 51:280–301. [PubMed: 11054877]

Belvindrah R, Nalbant P, Ding S, Wu C, Bokoch GM, Muller U. Integrin-linked kinase regulates Bergmann glial differentiation during cerebellar development. Mol Cell Neurosci. 2006; 33:109–25. [PubMed: 16914328]

Blaess S, Graus-Porta D, Belvindrah R, Radakovits R, Pons S, Littlewood-Evans A, Senften M, Guo H, Li Y, Miner JH, Reichardt LF, Muller U. Beta1-integrins are critical for cerebellar granule cell precursor proliferation. J Neurosci. 2004; 24:3402–12. [PubMed: 15056720]

Cellerino A, Pinzon-Duarte G, Carroll P, Kohler K. Brain-derived neurotrophic factor modulates the development of the dopaminergic network in the rodent retina. J Neurosci. 1998; 18:3351–62. [PubMed: 9547243]

Colognato H, Yurchenco PD. Form and function: the laminin family of heterotrimers. Dev Dyn. 2000; 218:213–34. [PubMed: 10842354]

Connolly SE, Hores TA, Smith LE, D'Amore PA. Characterization of vascular development in the mouse retina. Microvasc Res. 1988; 36:275–90. [PubMed: 2466191]

Deiner MS, Kennedy TE, Fazeli A, Serafini T, Tessier-Lavigne M, Sretavan DW. Netrin-1 and DCC mediate axon guidance locally at the optic disc: loss of function leads to optic nerve hypoplasia. Neuron. 1997; 19:575–89. [PubMed: 9331350]

Egles C, Claudepierre T, Manglapus MK, Champliaud MF, Brunken WJ, Hunter DD. Laminins containing the beta2 chain modulate the precise organization of CNS synapses. Mol Cell Neurosci. 2006

Fruttiger M. Development of the retinal vasculature. Angiogenesis. 2007; 10:77–88. [PubMed: 17322966]

Fujita M, Khazenzon NM, Bose S, Sekiguchi K, Sasaki T, Carter WG, Ljubimov AV, Black KL, Ljubimova JY. Overexpression of beta1-chain-containing laminins in capillary basement membranes of human breast cancer and its metastases. Breast Cancer Res. 2005; 7:R411–21. [PubMed: 15987446]

Gersdorff N, Kohfeldt E, Sasaki T, Timpl R, Miosge N. Laminin gamma3 chain binds to nidogen and is located in murine basement membranes. J Biol Chem. 2005; 280:22146–53. [PubMed: 15824114]

Goldowitz D, Hamre K. The cells and molecules that make a cerebellum. Trends Neurosci. 1998; 21:375–82. [PubMed: 9735945]

Graus-Porta D, Blaess S, Senften M, Littlewood-Evans A, Damsky C, Huang Z, Orban P, Klein R, Schittny JC, Muller U. Beta1-class integrins regulate the development of laminae and folia in the cerebral and cerebellar cortex. Neuron. 2001; 31:367–79. [PubMed: 11516395]

Hallmann R, Horn N, Selg M, Wendler O, Pausch F, Sorokin LM. Expression and function of laminins in the embryonic and mature vasculature. Physiol Rev. 2005; 85:979–1000. [PubMed: 15987800]

Harlow, E.; Lane, D. Antibodies: a laboratory manual. Cold Spring Harbor Laboratory; Cold Spring Harbor, NY: 1988.

Haverkamp S, Wassle H. Immunocytochemical analysis of the mouse retina. J Comp Neurol. 2000; 424:1–23. [PubMed: 10888735]

Hopker VH, Shewan D, Tessier-Lavigne M, Poo M, Holt C. Growth-cone attraction to netrin-1 is converted to repulsion by laminin-1. Nature. 1999; 401:69–73. [PubMed: 10485706]

Iivanainen A, Morita T, Tryggvason K. Molecular cloning and tissue-specific expression of a novel murine laminin γ3chain. J Biol Chem. 1999; 274:14107–11. [PubMed: 10318827]

Ido H, Ito S, Taniguchi Y, Hayashi M, Sato-Nishiuchi R, Sanzen N, Hayashi Y, Futaki S, Sekiguchi K. Laminin isoforms containing the γ3 chain are unable to bind to integrins due to the absence of the glutamic acid residue conserved in the C-terminal regions of the γ1 and γ2 chains. J Biol Chem. 2008; 283:28149–57. [PubMed: 18697739]

Iozzo RV, Cohen IR, Grassel S, Murdoch AD. The biology of perlecan: the multifaceted heparan sulphate proteoglycan of basement membranes and pericellular matrices. Biochem J. 1994; 302(Pt 3):625–39. [PubMed: 7945186]

Johnson J, Sherry DM, Liu X, Fremeau RT Jr, Seal RP, Edwards RH, Copenhagen DR. Vesicular glutamate transporter 3 expression identifies glutamatergic amacrine cells in the rodent retina. J Comp Neurol. 2004; 477:386–98. [PubMed: 15329888]

Koch M, Murrell JR, Hunter DD, Olson PF, Jin W, Keene DR, Brunken WJ, Burgeson RE. A novel member of the netrin family, beta-netrin, shares homology with the beta chain of laminin: identification, expression, and functional characterization. J Cell Biol. 2000; 151:221–34. [PubMed: 11038171]

Koch M, Olson PF, Albus A, Jin W, Hunter DD, Brunken WJ, Burgeson RE, Champliaud MF. Characterization and expression of the laminin gamma3 chain: a novel, non-basement membrane-associated, laminin chain. J Cell Biol. 1999; 145:605–18. [PubMed: 10225960]

Lewandoski M, Meyers EN, Martin GR. Analysis of Fgf8 gene function in vertebrate development. Cold Spring Harb Symp Quant Biol. 1997; 62:159–68. [PubMed: 9598348]

Libby RT, Champliaud MF, Claudepierre T, Xu Y, Gibbons EP, Koch M, Burgeson RE, Hunter DD, Brunken WJ. Laminin expression in adult and developing retinae: evidence of two novel CNS laminins. J Neurosci. 2000; 20:6517–28. [PubMed: 10964957]

Libby RT, Xu Y, Selfors LM, Brunken WJ, Hunter DD. Identification of the cellular source of laminin beta2 in adult and developing vertebrate retinae. J Comp Neurol. 1997; 389:655–67. [PubMed: 9421145]

Liesi P, Fried G, Stewart RR. Neurons and glial cells of the embryonic human brain and spinal cord express multiple and distinct isoforms of laminin. J Neurosci Res. 2001; 64:144–67. [PubMed: 11288143]

McGowan KA, Marinkovich MP. Laminins and human disease. Microsc Res Tech. 2000; 51:262–79. [PubMed: 11054876]

Mills J, Niewmierzycka A, Oloumi A, Rico B, St-Arnaud R, Mackenzie IR, Mawji NM, Wilson J, Reichardt LF, Dedhar S. Critical role of integrin-linked kinase in granule cell precursor proliferation and cerebellar development. J Neurosci. 2006; 26:830–40. [PubMed: 16421303]

Miner JH, Cunningham J, Sanes JR. Roles for laminin in embryogenesis: exencephaly, syndactyly, and placentopathy in mice lacking the laminin alpha5 chain. J Cell Biol. 1998; 143:1713–23. [PubMed: 9852162]

Miner JH, Li C. Defective glomerulogenesis in the absence of laminin alpha5 demonstrates a developmental role for the kidney glomerular basement membrane. Dev Biol. 2000; 217:278–89. [PubMed: 10625553]

Mountford P, Zevnik B, Duwel A, Nichols J, Li M, Dani C, Robertson M, Chambers I, Smith A. Dicistronic targeting constructs: reporters and modifiers of mammalian gene expression. Proc Natl Acad Sci U S A. 1994; 91:4303–7. [PubMed: 8183905]

Noakes PG, Gautam M, Mudd J, Sanes JR, Merlie JP. Aberrant differentiation of neuromuscular junctions in mice lacking s-laminin/laminin beta 2. Nature. 1995; 374:258–62. [PubMed: 7885444]

O'Roak BJ, Deriziotis P, Lee C, Vives L, Schwartz JJ, Girirajan S, Karakoc E, Mackenzie AP, Ng SB, Baker C, Rieder MJ, Nickerson DA, Bernier R, Fisher SE, Shendure J, Eichler EE. Exome sequencing in sporadic autism spectrum disorders identifies severe de novo mutations. Nature Genetics. 2011; 43:585–589. [PubMed: 21572417]

Sanes JR, Engvall E, Butkowski R, Hunter DD. Molecular heterogeneity of basal laminae: isoforms of laminin and collagen IV at the neuromuscular junction and elsewhere. J Cell Biol. 1990; 111:1685–99. [PubMed: 2211832]

Schneiders FI, Maertens B, Bose K, Li Y, Brunken WJ, Paulsson M, Smyth N, Koch M. Binding of netrin-4 to laminin short arms regulates basement membrane assembly. J Biol Chem. 2007; 282:23750–23758. [PubMed: 17588941]

Schymeinsky J, Nedbal S, Miosge N, Poschl E, Rao C, Beier DR, Skarnes WC, Timpl R, Bader BL. Gene structure and functional analysis of the mouse nidogen-2 gene: nidogen-2 is not essential for basement membrane formation in mice. Mol Cell Biol. 2002; 22:6820–30. [PubMed: 12215539]

Siu MK, Cheng CY. Interactions of proteases, protease inhibitors, and the beta1 integrin/laminin gamma3 protein complex in the regulation of ectoplasmic specialization dynamics in the rat testis. Biol Reprod. 2004; 70:945–64. [PubMed: 14645107]

Smyth N, Vatansever HS, Murray P, Meyer M, Frie C, Paulsson M, Edgar D. Absence of basement membranes after targeting the LAMC1 gene results in embryonic lethality due to failure of endoderm differentiation. J Cell Biol. 1999; 144:151–60. [PubMed: 9885251]

Sorokin L, Girg W, Gopfert T, Hallmann R, Deutzmann R. Expression of novel 400-kDa laminin chains by mouse and bovine endothelial cells. Eur J Biochem. 1994; 223:603–10. [PubMed: 8055931]

Sorokin LM, Pausch F, Frieser M, Kroger S, Ohage E, Deutzmann R. Developmental regulation of the laminin alpha5 chain suggests a role in epithelial and endothelial cell maturation. Dev Biol. 1997; 189:285–300. [PubMed: 9299121]

Sugiyama S, Utani A, Yamada S, Kozak CA, Yamada Y. Cloning and expression of the mouse laminin gamma 2 (B2t) chain, a subunit of epithelial cell laminin. Eur J Biochem. 1995; 228:120–8. [PubMed: 7882992]

Sunada Y, Bernier SM, Kozak CA, Yamada Y, Campbell KP. Deficiency of merosin in dystrophic dy mice and genetic linkage of laminin M chain gene to dy locus. J Biol Chem. 1994; 269:13729–32. [PubMed: 8188645]

Thyboll J, Kortesmaa J, Cao R, Soininen R, Wang L, Iivanainen A, Sorokin L, Risling M, Cao Y, Tryggvason K. Deletion of the laminin alpha4 chain leads to impaired microvessel maturation. Mol Cell Biol. 2002; 22:1194–202. [PubMed: 11809810]

Tunggal P, Smyth N, Paulsson M, Ott MC. Laminins: structure and genetic regulation. Microsc Res Tech. 2000; 51:214–27. [PubMed: 11054872]

Weller M, Krautler N, Mantei N, Suter U, Taylor V. Jagged1 ablation results in cerebellar granule cell migration defects and depletion of Bergmann glia. Dev Neurosci. 2006; 28:70–80. [PubMed: 16508305]

Wilson BD, Ii M, Park KW, Suli A, Sorensen LK, Larrieu-Lahargue F, Urness LD, Suh W, Asai J, Kock GA, Thorne T, Silver M, Thomas KR, Chien CB, Losordo DW, Li DY. Netrins promote developmental and therapeutic angiogenesis. Science. 2006; 313:640–4. [PubMed: 16809490]

Yan HH, Cheng CY. Laminin alpha 3 forms a complex with beta3 and gamma3 chains that serves as the ligand for alpha 6beta1-integrin at the apical ectoplasmic specialization in adult rat testes. J Biol Chem. 2006; 281:17286–303. [PubMed: 16608848]

Yin Y, Kikkawa Y, Mudd JL, Skarnes WC, Sanes JR, Miner JH. Expression of laminin chains by central neurons: analysis with gene and protein trapping techniques. Genesis. 2003; 36:114–27. [PubMed: 12820173]

Yurchenco PD, Wadsworth WG. Assembly and tissue functions of early embryonic laminins and netrins. Curr Opin Cell Biol. 2004; 16:572–9. [PubMed: 15363809]

Zenker M, Aigner T, Wendler O, Tralau T, Muntefering H, Fenski R, Pitz S, Schumacher V, Royer-Pokora B, Wuhl E, Cochat P, Bouvier R, Kraus C, Mark K, Madlon H, Dotsch J, Rascher W, Maruniak-Chudek I, Lennert T, Neumann LM, Reis A. Human laminin beta2 deficiency causes congenital nephrosis with mesangial sclerosis and distinct eye abnormalities. Hum Mol Genet. 2004; 13:2625–32. [PubMed: 15367484]

Highlights

This study documents the developmental expression of the γ3 chain of laminin in the mouse.

γ3 is expressed in a wide variety of basement membranes; including brain and retinal vasculature, cerebellum, kidney, testis and skin. No expression was noted in the vasculature outside the brain or retina

γ3 reactive antibodies were produced and characterized.

Lamc3 null mouse was generated and the phenotype characterized.

The Lamc3 null mouse is viable, lives normal lifespan, had no defects in skin, hair, or retinal structure or function.

The Lamc3 null mouse has disrupted cerebellar formation.

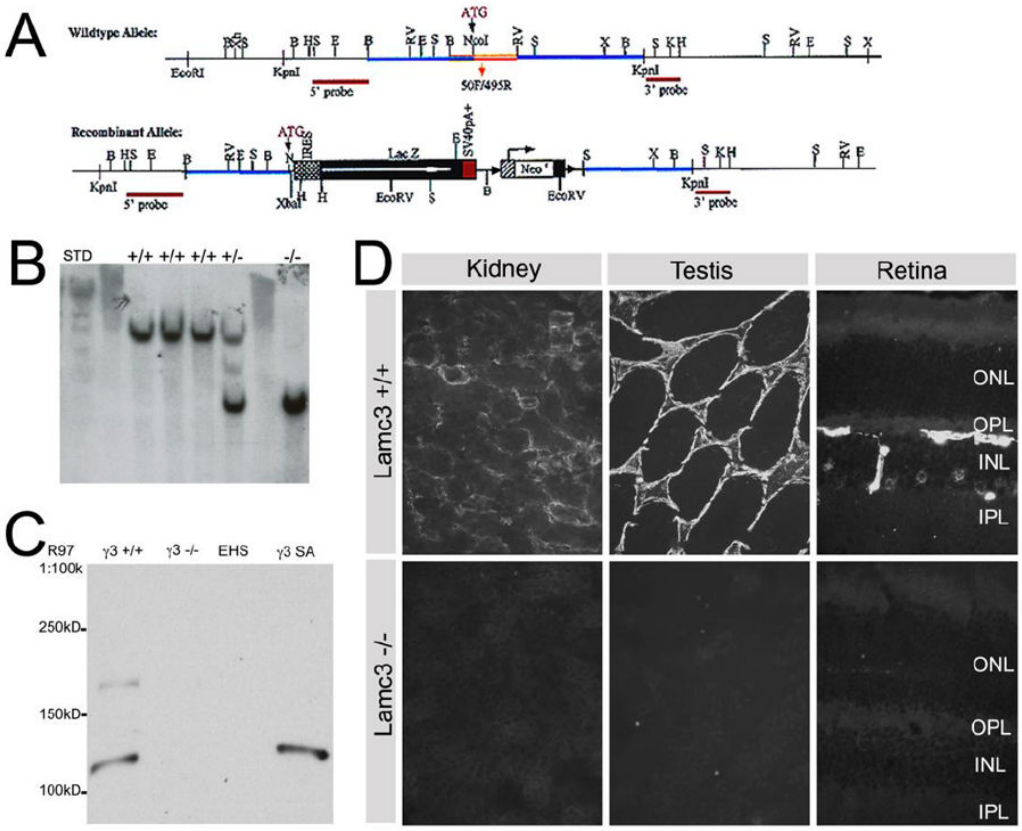

Figure 1.

Generation and verification of *Lamc3-/-* mice. A: A schematic view of *Lamc3* wild type and recombinant alleles. The targeting construct was created by cloning a 3.6kb BamHI fragment containing the promoter and 5′ UTR of the *Lamc3* gene together with the SalI fragment of pGT1.8 Ires βgeo (Mountford et al., 1994) and a 4.3kb EcoRV-KpnI fragment of intron 1 of *Lamc3*. The resulting targeting vector created a 2.2kb deletion spanning exon 1 and part of intron 1 of the *Lamc3* gene and replaced with a promoter-less IRES β-Geo cassette. The neo cassette was subsequently removed. B: Southern blot screening of HindIII digests of genomic DNA for *Lamc3*+/+, *Lamc3*+/- and *Lamc3-/-* mice, probed with the "5' probe". The endogenous allele is present as a ~10.5 kb band; the recombinant allele is present as a ~5.9 kb band. C: Western blot of *Lamc3*+/+ (γ3+/+) and *Lamc3-/-* (γ3-/-) retina homogenates using the γ3 chain antiserum R97. EHS laminin (EHS) and recombinant γ3 chain short arm protein (γ3SA) were controls. R97 reacted with γ3SA at about 120kD. R97 also reacted with bands of 120kD and 180kD in the wild-type (γ3+/+). No reactivity was observed with *Lamc3-/-* homogenates (γ3-/-) or with EHS laminin. D: Immunohistological staining of *Lamc3*+/+ and *Lamc3-/-* kidney, testis and retina using anti-γ3 chain antibody R96. There was no detectable laminin γ3 IR in the *Lamc3-/-* tissues.

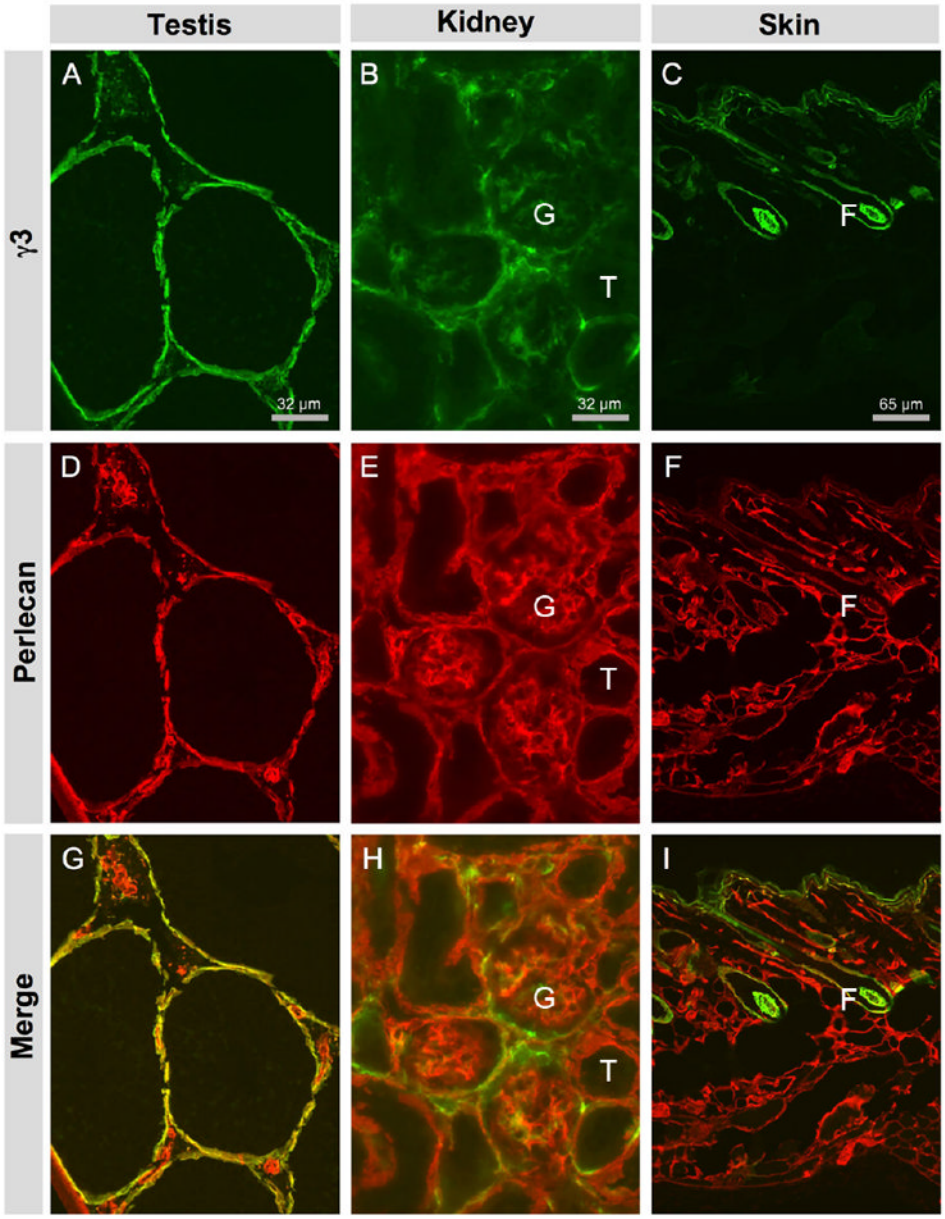

Figure 2.

Laminin γ3 chain is widely but unevenly distributed in the basement membranes of various tissues. A, D, G: testis. B, E, H: kidney. C, F, I: skin. A, B, C: γ3 IR in testis, kidney and skin, respectively. D, E, F: Perlecan IR marks the BMs in these tissues. G, H, I: Overlay of γ3 IR and perlecan IR. A: In testis, γ3 IR is mainly located at the BM of seminiferous tubes; some γ3 IR is located at the BM of interstitial structures, presumably vasculature. D: In testis, perlecan IR is more broadly distributed. B: In kidney, γ3 IR is present mainly in glomerular (G) BM and somewhat weakly and discontinuously in the tubular (T) BM. E: In kidney, perlecan IR is evenly distributed in the BMs of kidney tubules and in the GBM. C: In skin, γ3 IR is located at the BM of the epidermis and around the hair follicle (F). F: In skin, perlecan is more widely distributed throughout the skin.

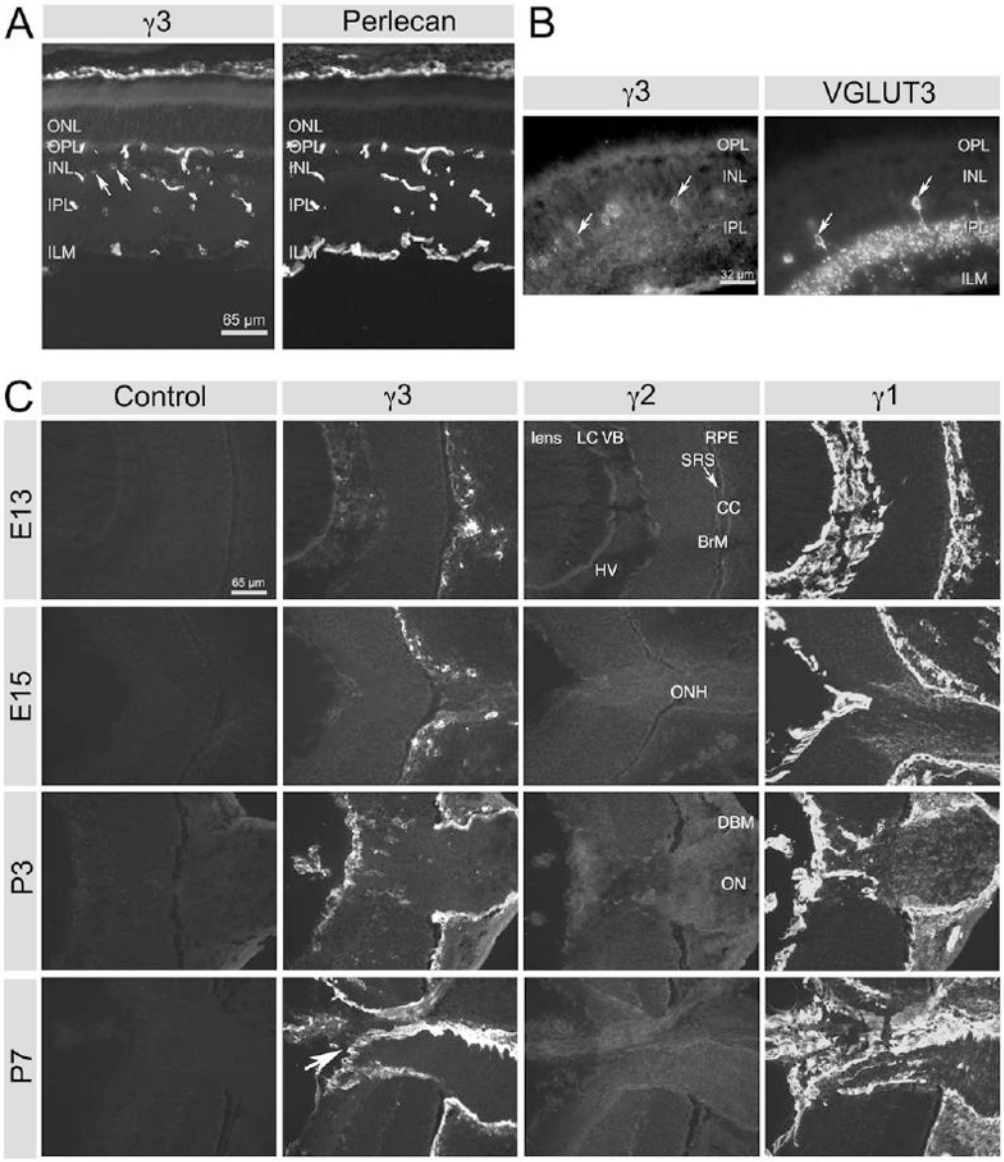

Figure 3.

Spatial and developmental expression of laminin γ chains in the retina. A: In alcohol-fixed tissue, laminin γ3 chain IR is mainly located in vascular BMs and Bruch's membrane. Very little laminin γ3 chain IR is found in the inner limiting membrane (ILM) as well as some cells in the inner nuclear layer (INL; arrows). All BMs display uniform perlecan IR. ONL, outer nuclear layer; OPL, outer plexiform layer; IPL, inner plexiform layer. B: In PFA-treated tissue, VGLUT3-expressing amacrine cells (arrows) also have laminin γ3 chain IR. C: All three laminin γ chains were studied during development in alcohol-fixed tissue. Laminin γ2 chain was only weakly detectable at any stage; laminin γ1 chain is widely expressed in the basement membranes of the lens and the retina (Bruch's membrane and the ILM) as well as in the vitreous. Throughout development (from E13 to P7), γ1 is the predominant γ chain in the BMs of the retina and γ1 is also expressed in the optic nerve as part of the neurolemma. The γ3 chain's distribution coincides with the γ1 chain's distribution only in some regions, but γ3 is a prominent component of the BMs of the developing retinal vasculature (arrow at P7; see text for full details). Labels in γ2 sections

apply to all sections in C: LC, lens capsule; VB, vitreous body; RPE, retinal pigmented epithelium; SRS, sub-retinal space; CC, choriocapillaris; BrM, Bruch's membrane; HV, hyaloid vessels; ONH, optic nerve head; DBM, dural basement membrane; ON, optic nerve.

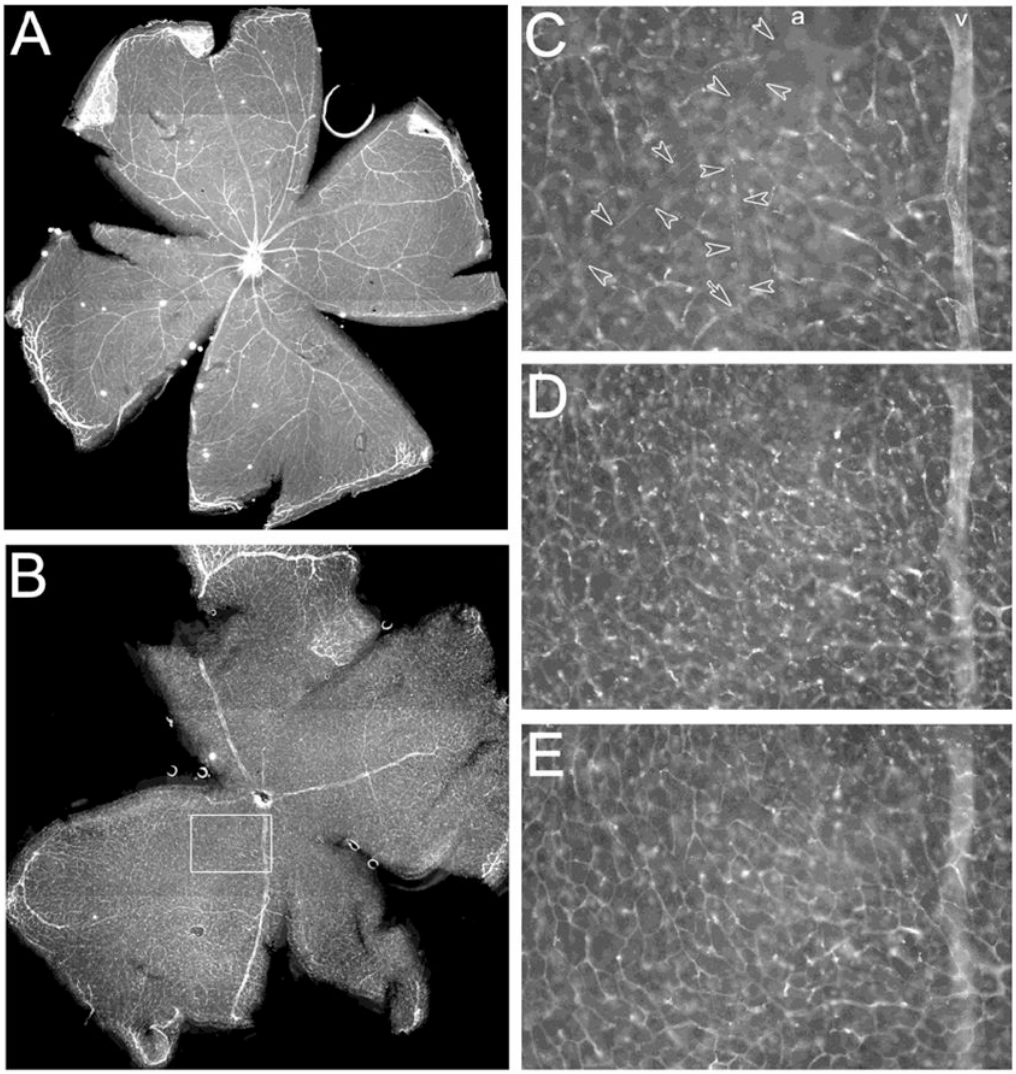

Figure 4.

Laminin γ1 and 3 chains in retinal vascular basement membrane. A: Laminin γ1 chain is deposited in the BMs of both arteries and veins in the retina. B: Laminin γ3 chain is deposited in the BMs of veins and microvessels but not arteries. C-E: Different focal planes of the boxed area in B. C: The vitreal surface of the retina; γ3 IR is present in veins (v) but not in arteries (a, marked by the empty arrow heads) and surface capillaries. D: The INL; γ3 IR is present in neurons and capillary basement membranes. E: The OPL; γ3 IR is present in the capillary bed.

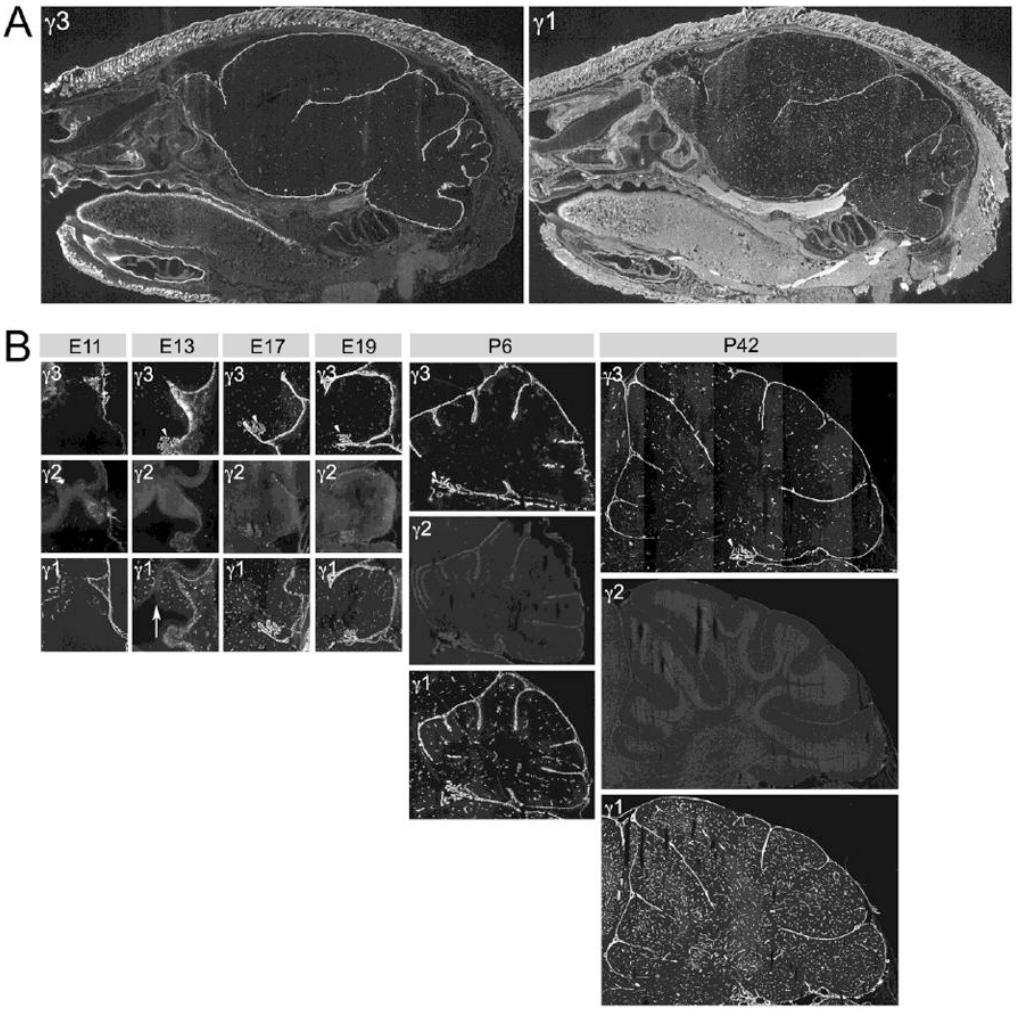

Figure 5.

Spatial and developmental expression of laminin γ chains in the brain. A: Sagittal sections of P6 mouse head. Adjacent sections reacted with laminin γ3 and γ1 antibodies, respectively. Laminin γ3 chain IR is present in various BMs of the brain, such as the pial and vascular BMs. Laminin γ1 chain IR is more widely distributed, not only in the CNS, particularly in the vasculature, but also in other tissues (e.g., the tongue). B: Developmental expression of all three laminin γ chains in the mouse cerebellum, from E11 through P42. Laminin γ3 chain IR is present in various BMs during development. Laminin γ2 chain IR is nearly absent at all ages. Laminin γ1 chain IR is most widely distributed at all ages. Arrowheads mark the choroid plexus; the arrow marks the ventricular zone. See text for details.

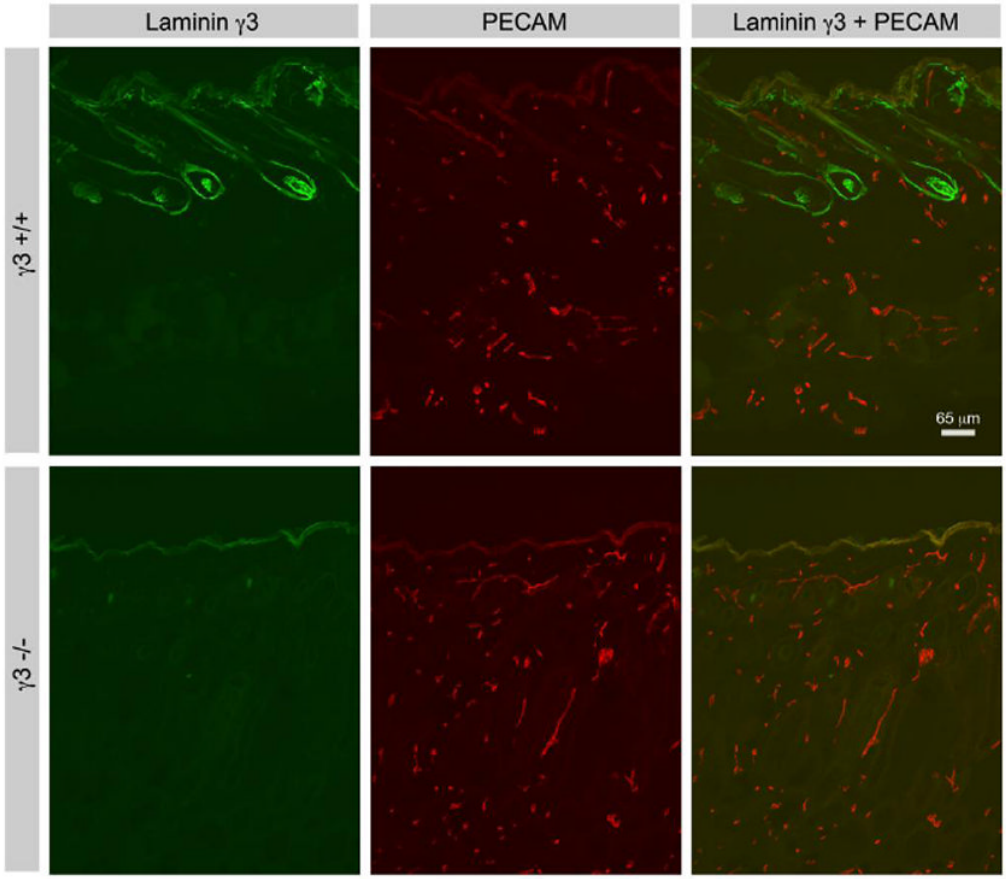

Figure 6.
Comparison of laminin γ3 chain and PECAM expression in *Lamc3*+/+ and *Lamc3*-/- skin. Laminin γ3 chain IR is prevalent in hair follicles and the basement membrane of the skin, but is absent from PECAM-expressing peripheral vessels. Laminin γ3 chain IR in the follicles and skin basement membrane is extinguished in *Lamc3*-/- skin.

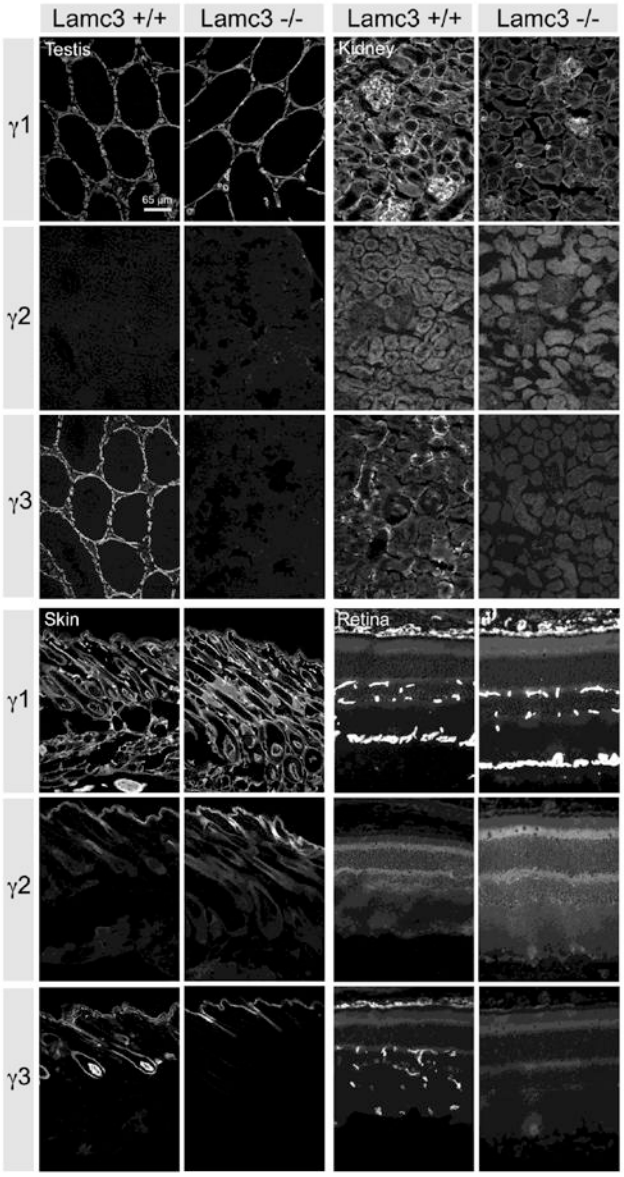

Figure 7.

Comparison of laminin γ chain expression in *Lamc3*+/+ and *Lamc3-/-* tissues. There is little or no change in laminin γ1 chain IR, and no obvious change of the laminin γ2 chain IR in the *Lamc3-/-* retina, kidney, testis and skin (see text for details).

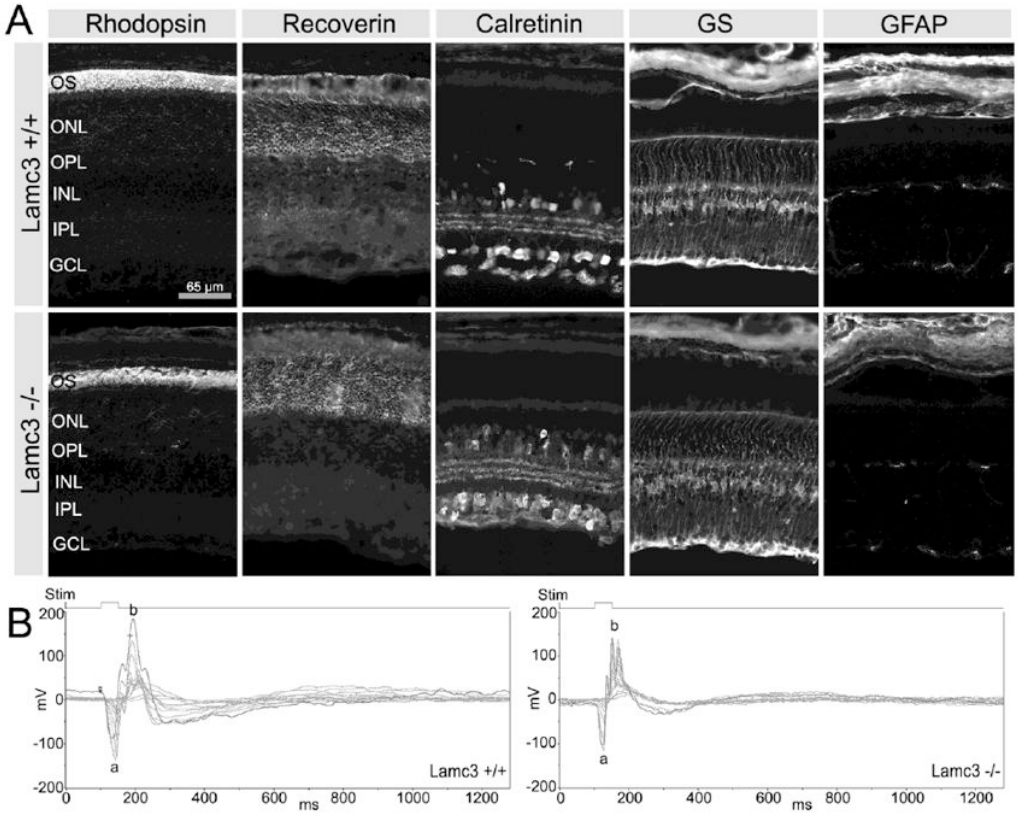

Figure 8.

Comparison of cell markers and ERGs in *Lamc3*+/+ and *Lamc3*-/- retinas. A: Photoreceptor outer segment (OS) labeled with anti-rhodopsin, photoreceptors labeled with anti-recoverin, amacrine cells labeled with anti-calretinin, Müller cells labeled with anti-glutamine synthetase (GS), and astrocytes labeled with anti-GFAP display no obvious differences between the *Lamc3*+/+ and *Lamc3*-/- retinas. B: The *Lamc3*-/- ERG has both a- and b-waves, although the amplitude of the *Lamc3*-/- b-wave is smaller than that in the *Lamc3*+/+. Thin lines, ERG traces of each trial; thick lines, the average of individual trials. Light flash (Stim), 50 ms.

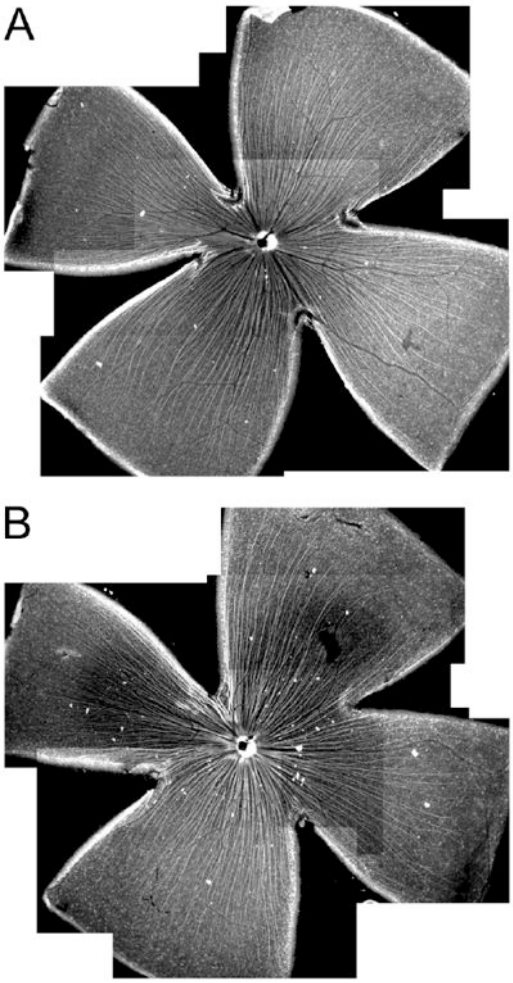

Figure 9.

The pathfinding of RGC axons to the optic nerve head in *Lamc3*+/+ and *Lamc3*-/- retinas. A: RGC axons labeled with anti-neurotubulin (TuJ-1) antibody run toward the optic nerve head in a whole-mounted *Lamc3*+/+ retina. B: RGC axon trajectory appears normal in the whole-mounted *Lamc3*-/- retina.

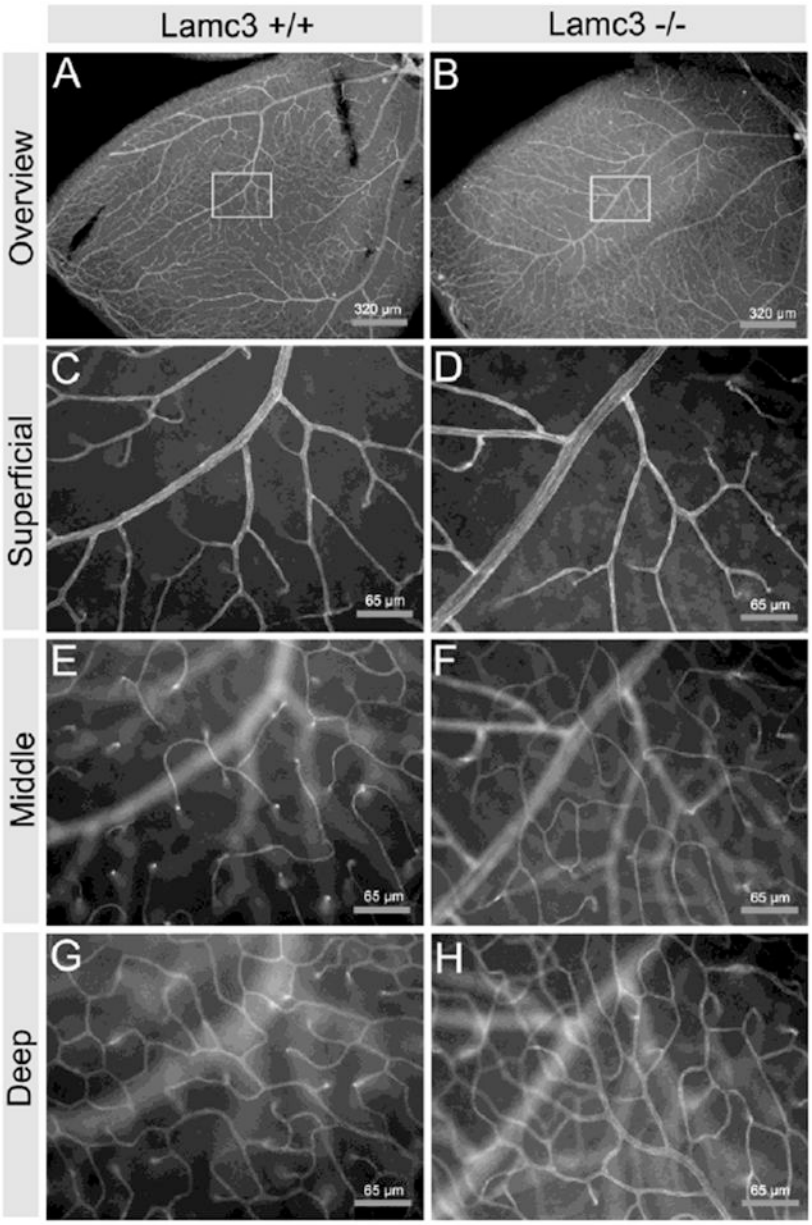

Figure 10.

Lamc3-/- retinas appear to have increased microvasculature. Retinal vasculature was visualized with an antibody to PECAM (CD31). A, C, E, G: *Lamc3+/+*. B, D, F, H: *Lamc3-/-*. A, B: Low magnification. C-H: Higher magnifications of the boxed areas in A and B. C, D: the focus is at the vitreal surface (Superficial). E, F: the focus is at the INL-IPL level (Middle). G, H: the focus is at the OPL level (Deep).

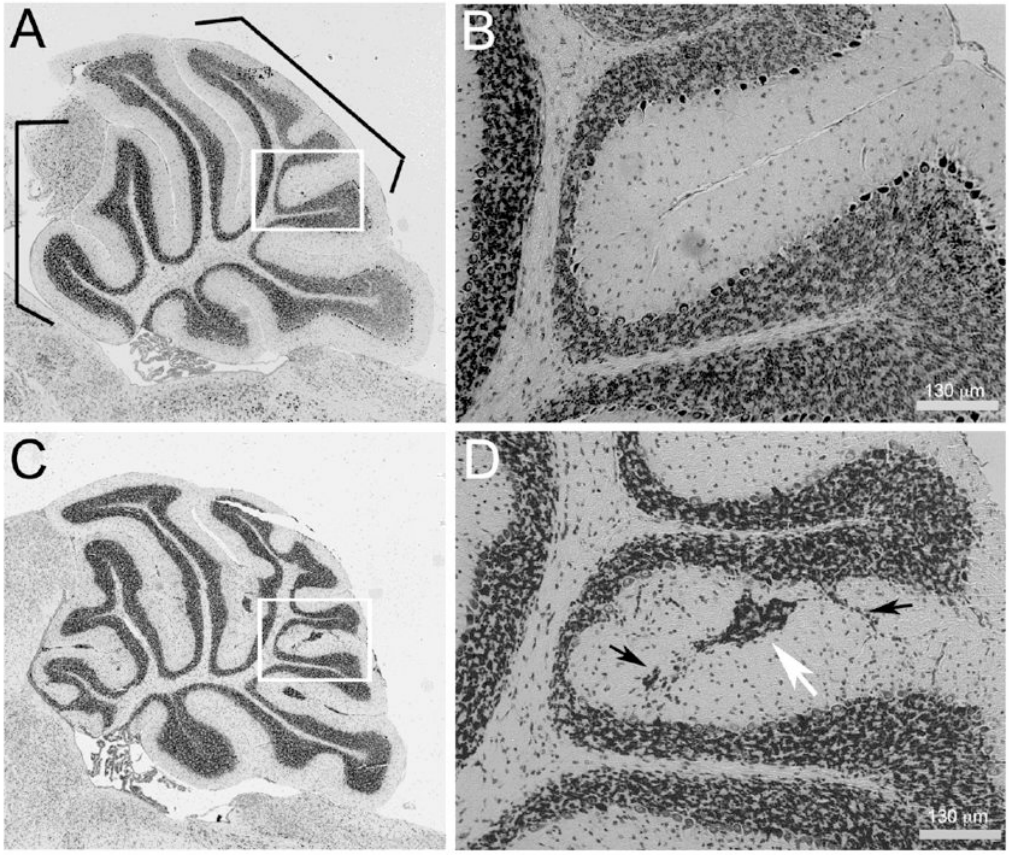

Figure 11.

Ectopic cells are present in the *Lamc3-/-* cerebellum. A: Mid-sagittal section of a *Lamc3+/+* cerebellum. B: Higher magnification of the boxed area in A. C: Mid-sagittal section of a *Lamc3-/-* cerebellum. The *Lamc3-/-* cerebellum has ectopic cells and an abnormal foliation pattern. D: Higher magnification of the boxed area in C. Streams (black arrows) and islands (white arrow) of ectopic cells are present in the molecular layer of the *Lamc3-/-* cerebellum.

Table 1

There was no significant change in γ1 mRNA level in retina or testis of the *Lamc3*+/+ and *Lamc3*-/- mice by QPCR.

	Retina		Testis	
	n	ΔCt	n	ΔCt
Lamc3+/+	7	15.5±1.8	2	11.9±0.5
Lamc3-/-	9	15.4±1.0	3	12.3±0.3